General Disclaimer

One or more of the Following Statements may affect this Document

- This document has been reproduced from the best copy furnished by the organizational source. It is being released in the interest of making available as much information as possible.
- This document may contain data, which exceeds the sheet parameters. It was furnished in this condition by the organizational source and is the best copy available.
- This document may contain tone-on-tone or color graphs, charts and/or pictures, which have been reproduced in black and white.
- This document is paginated as submitted by the original source.
- Portions of this document are not fully legible due to the historical nature of some
 of the material. However, it is the best reproduction available from the original
 submission.

Produced by the NASA Center for Aerospace Information (CASI)

Unclas 35920

63/44

(NASA-CR-162364) INVESTIGATION OF PROPOSED PROCESS SEQUENCE FOR THE ARRAY AUTOMATED ASSEMBLY TASK, PHASE 2 Quarterly Technical Progress Report, period ending 30 Jun. 1979 (Spectrolab, Inc.) 59 p HC A04/MF A01

QUARTERLY TECHNICAL PROGRESS REPORT

on the

INVESTIGATION OF PROPOSED PROCESS SEQUENCE FOR THE ARRAY AUTOMATED ASSEMBLY TASK - PHASE II

For Quarter Ending

June 30, 1979

JPL Contract 954853 CDRL 010

Prepared by:

Nick Mardesich Alec Garcia Steve Bunyan Angel Pepe

Approved by:

William E. Taylor, Manager Process Development and Engineerin

Process Development and Engineering

of

SPECTROLAB, INC. 12500 Gladstone Avenue Sylmar, CA 91342

July 1979

The JPL Low-Cost Silicon Solar Array Project is sponsored by the U. S. Department of Energy and forms part of the Solar Photovoltaic Conversion Program to initiate a major effort toward the development of low-cost solar arrays. This work was performed for the Jet Propulsion Laboratory, California Institute of Technology by agreement between NASA and DOE.

Table of Contents

Section 👙	<u>Title</u>	Page
1.0	SUMMARY	1
2.0	INTRODUCTION	3
3.0	TECHNICAL DISCUSSION	7
3.1	Surface Preparation	7
3.2	Junction Formation	7
3.3	Back Surface Field	15
3.3.1	Cell Bowing	15
3.3.2	Mesh Screen Sizing	20
3.4	Cleaning Prior to Front Metallization	20
3.5	Printed Silver Front Contact	22
3.6	Junction Isolation	30
3.7	AR Coating	36
3.8	Module Assembly	41
3.8.1	Lamination	41
3.8.2	Interconnections	43
4.0	CONCLUSIONS	47
5,0	RECOMMENDATIONS	49
6.0	NEW TECHNOLOGY	49
Appendix 1.	Series Resistance Calculations for Front Ohmic	50
Appendix 2.	Series Resistance Calculations for Interconnects	56

NOTICE

A recalibration of our tungsten lighthouse has shown it to be out of calibration. Short circuit current and load point current data should be reduced by 7% in quarterly reports for quarters ending September 1978 and March 1979.

1.0 SUMMARY

Evaluation of (110) wafers have shown partial surface texturing occurs in our normal 30% NaOH surface preparation.

Tests of polymeric diffusion sources indicate PX-10 to be superior to N-250, but the Paasche air brush application is unable to produce uniform thicknesses. A uniform thickness of PX-10 was achieved with a spin-on technique. Tests indicate diffusion with PX-10 at $900 \pm 25^{\circ}$ C to be very acceptable in producing good quality cells.

Cells produced with patterned aluminum back appear to be effective in reducing bowing effects without any obvious loss in cell performance.

Cells with high series resistance are being produced with our present front silver grid pattern (1 mil emulsion screen). The Major contribution to this resistance comes from the center ohmic bar.

Evaluation of a two mil emulsion on our front silver grid screens indicates effectiveness in reducing series resistance, but clogging problems appear in screen printing through the 6 mil wide grid lines. Measurements of our modified thick film systems paste indicate a resistivity of 2.6 times that of bulk silver.

Preliminary application of laser scribing and cleaving appears to give a reliable method of junction removal as compared to junction removal with a chemical edge etch.

Preliminary results of spray-on titanium isopropoxide AR coating, with the Advanced Concept Spray System, indicate as high as 31% increase in efficiency.

Interconnect material has been procured and power losses due to series resistance calculated. Power loss in the 2' x 4' module planned for verification test was estimated to be 0.3 watts maximum.

The process step of ultrasonically soldering a tin pad for back contacts has been resequenced into the circuit fabrication process in module fabrication. The tin pad is now applied at the same time the cell string is fabricated. This technique resulted in interconnect pull strength of greater than 700 grams.

Small test laminations have been successfully processed with A-8914-2 EVA in a nylon bagging material. A suitably rigid material under the nylon appears to be necessary to avoid bubbles and ripples in the EVA.

2.0 INTRODUCTION

This Quarterly Technical Progress Report covers the quarter ending June 30, 1979. The scope of the contract covers the investigation of technology readiness of a proposed process sequence for the low cost fabrication of photovoltaic modules as part of the Phase 2 of the Array Automated Assembly Task, Large Solar Array project.

The cell and module process sequence is shown in Table 2.0-1. The baseline process is defined by the heavy line. This process sequence was shown to be technically feasible and cost effective during the first half of the Phase 2 effort, either by Spectrolab or by other contractors. There is, however, the opportunity and need for further process improvement of some of the steps. In some cases alternative processes may be more cost effective than those in the baseline sequence. These are indicated in Table 2.0-1 by the alternative routes marked with solid light lines. The dotted line routes are fall-back routes in case the baseline sequence encounters insolvable problems.

The process sequence presumes that the input sheet material will be in a form not suitable for texture etching. A brief plasma etch will be evaluated as a means of establishing a standard surface for input to the process sequence. The junction will be formed by diffusion from an N-type polymeric spray-on source. A P+ back contact will be formed by firing a screen printed aluminum paste. After cleaning the back aluminum and removing the diffusion oxide, screen printed front contacts will be formed. The junction will be cleaned by a laser scribe operation and an AR coating formed by baking a suitable polymeric spray-on film.

A process step for applying a tin pad ultrasonically to the aluminum back has been resequenced into the module assembly sequence. At the point of assembling series strings the cells will be tin padded and interconnected simultaneously.

Table 2.0-1
PROCESS SEQUENCE

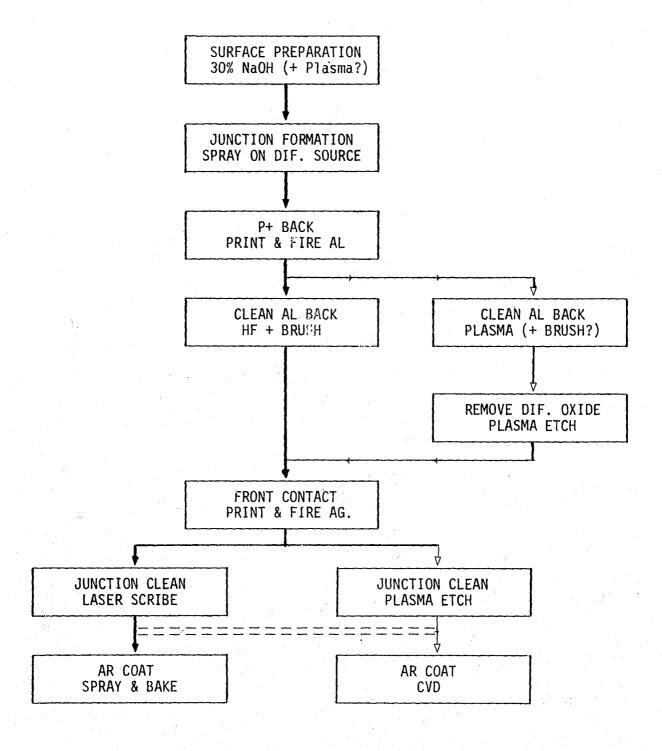
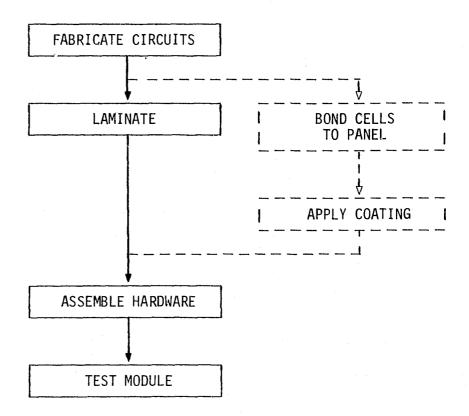


Table 2.0-1 (continued)



Cell strings will be assembled into solar circuits and laminated to superstrates or substrates, preferably using ethylene vinyl acetate as an encapsulant and laminating medium. After assembling the frame and termination hardware, the finished module will be tested.

During the period reported here work has continued on integrating the "Junction Clean" and "AR Coat" process steps into the total sequence. The "Junction Formation" step is being further opt mized. In the module area all steps of the baseline process have been successfully integrated to produce a 12" x 15" module.

In view of successful results with the baseline cell process sequence, an alternative fall-back sequence involving a boron diffused P+ back surface field has been abandoned.

3.0 TECHNICAL DISCUSSION

3.1 SURFACE PREPARATION

Ingots procured from Wacker (10 ohm-cm) have been sectioned into 2.125" cubes and sliced to produce wafers with a (110) surface orientation. The normal 30% NaOH etching treatment for 20 minutes resulted in removing 6 mils from the surface. (100) wafers generally lose 3 mils in 20 minutes. This treatment produced a slight textured surface. This surface preparation would produce an irregular surface if applied to EFG ribbons or polycrystalline wafers since these materials have many surface orientations.

In run 5.46.9 (110) Wacker wafers were etched in 30% NaOH for 10 minutes and processed in accordance with our baseline process, Table 2.0-1, except the junction was cleaned by chemical etching and some wafers were evaporated with SiO_X to produce an AR coating. Three different ingots were processed with practically the same results. The cell conversion efficiencies were 10.0%, 9.7% and 9.7%. Some of these cells were AR coated with SiO_X, which increased the efficiency 24 to 28%. Nontextured cells normally increase about 34%. The 30% NaOH treatment on the (110) surface produces a semi-textured surface resulting in the smaller incremental increase with AR coating.

3.2 JUNCTION FORMATION

During this period experiments were continued to improve diffusion and to optimize parameters for the N-250 and PX-10 sources, to explore the effects of process variations and to verify the previously observed superior performance of the PX-10 source. In the first experiment cells were fabricated using our baseline process sequence (Table 2.0-1).

NaOH polished 2" round wafers were used to compare N-250 and PX-10. The PX-10 gave the best results. The average open circuit voltage was 604 mV and the average load point current (I_{500}) was 432 mA for 19 of 20 cells. For the N-250 the average open circuit voltage was 602 mV and the average load point current (I_{500}) was 409 mA for 14 of 20 cells.

As a further test of the PX-10 and N-250 an experiment was run varying the applied thickness of PX-10. In run 4.27.9 a thin spray-on coat of PX-10, a thick coat of PX-10 and a normal coat of N-250 were applied on 2.12 x 2.12 inch square NaOH polished wafers. The cells were processed in accordance with the proposed sequence except that the junctions were cleaned chemically and the wafers were not AR coated.

The results of this run gave efficiencies of 8.6% (equivalent to 11.5% with AR coating), 10.4% (= 13.9% with AR coating) and 8.4% (= 11.1% with AR coating) for the average efficiency of the thin PX-10, thick PX-10 and N-250, respectively (Table 3.2-1). The performance of cells with thinly applied PX-10 may be low due to a non-uniform diffusion which is indicated by the lower shunt resistance, although the sheet resistance of diffused wafers for both the thin and thick PX-10 appeared the same. Some cells produced with the thick spray-on PX-10 source showed areas of source remaining after the HF treatment. These layers may be acting as an antireflective coating in these areas, resulting in increasing the short circuit current and current at load. This is consistent with the visual evidence, that the cells with spotty surfaces generally have higher short circuit currents. Comparison of the two diffusion sources is confused because the performance characteristics of the deeply diffused N-250 group are suspect, the reason being the tungsten light source spectrum used to characterize the cells is not influenced by deep junction as much as a true AM1 solar spectrum would be.

Table 3.2-1

Run 4.27.9
PX-10 SPRAYING THICKNESS EFFECTS

No AR Coating 2.12" x 2.12" Cells

	AVERAGE					
	V (mV)	I sc (mA)	I ₅₀₀ (mA)	R _{sh}		
Thin PX-10	605	681	500	19.4		
Thick PX-10	605	708	560	17.8		
N-250	599	621	485	11.0		

The method of applying the PX-10 source by air brush may be contributing to the problem. Air brush application may not produce a sufficiently uniform coating. Spinning-on PX-10 appears to give a thin uniform layer of source which results in a wafer surface which is easily cleaned with an HF treatment. To compare effects of different methods of applying PX-10, cells were fabricated by spraying-on and spinning-on the diffusion source to a 3" round wafer with a NaOH polished (non-textured) surface. After the P+ formation and aluminum back contact, a 2" x 2" square wafer was cut out. Cutting the square wafers out, chemically cleaning the junction, and no AR coating were the only deviations from the baseline process. The spin-on appeared more uniform but was lower in output at load point current I 500. average open circuit voltage was 602 mV with the highest being 604 mV, and the average load point current (I_{500}) was 531 mA with the highest being 575 mA.

At this time PX-10 appeared superior to N-250 because it produced superior performance and also had a shorter diffusion time cycle. Additional experiments were then performed to explore the time-temperature response surface for diffusion with the PX-10 diffusion source. The cells were fabricated using the baseline process sequence except the wafers were sectioned by laser scribing prior to front metallization and no AR coating was applied. The diffusion source was applied by spinning because of lack of suitable spray equipment.

Baseline diffusion of 10 minutes N_2 and then 5 minutes O_2 at $900^{\circ} c$ was performed in run 4.30.9. The average efficiency of this run was 10.0 (equivalent to 13.3% with AR coating). A diffusion time of 10 minutes in N_2 and 5 minutes in O_2 was selected in run 4-31-9 while the temperature was varied between 850 and $925^{\circ} C$ in $25^{\circ} C$ intervals. The average efficiencies for this run were 7.1% (= 9.8% with AR coating), 8.6% (= 11.6% with AR coating), 9.3% (= 12.5%

with AR coating), for the 850, 875, 900 and 925°C diffusion temperatures, respectively. The control group of 900°C was about 10% lower than run 4.30.9. This drop was traced to the diffusion source being spun-on and dried the night before the diffusion occurred.

Run 4.31.9 was repeated in 4.33.9, and the source was diffused within one hour of source application. The average efficiencies were 9.2% (=12.3% with AR coating), 10.0% (=13.4% with AR coating) and 9.9 (=13.2 with AR coating) for the 850, 875, 900 and 925°C diffusion temperatures, respectively. The control group of 900°C was the same as run 4.20.9. The three temperatures of 875, 900 and 925°C appear to have similar efficiencies, but they do reflect a variation in sheet resistivity and short circuit current as a function of temperature.

As an additional verification of the 875, 900 and $925^{\circ}C$ temperature invariance, both the 875 (run 5.44.9) and $925^{\circ}C$ (run 5.41.9) were repeated in separate experiments using the $900^{\circ}C$ diffusion as a control. In run 5.44.9 the average efficiencies were 9.8% (=13.1% with AR coating) and 9.7% (=13.2% with AR coating) for the 875 and $900^{\circ}C$ (control) diffusion temperatures, respectively. In run 5.41.9 the average efficiencies were 9.2% (=12.0% with AR coating) and 9.2% (=12.0% with AR coating) for the 900 (control) and $925^{\circ}C$ diffusion temperatures, respectively. Although the performance does not appear to be strongly temperature dependent in the $900 \pm 25^{\circ}C$ range, there does appear to be a short circuit current dependence. The temperature dependence of performance at load may be masked by the low shunt resistance in these runs. Results of these experiments are summarized in Table 3.2-2.

In view of the resistance effects, two more experiments were run: 6.48.9 and 6.51.9. Tables 3.2-3 and 3.2-4 show a summarization of the results. Looking at the results of these experiments in contrast to the previous experiments, there are differences among

Table 3.2-2

JUNCTION FORMATION EXPERIMENTS

				Average	e Value			
Run No.	Temperature	Sheet (Ω/\Box)	V _{OC} (mV)	I _{sc}	^I 500 (mA)	R _{sh}	<u>η (ዩ)</u>	Equivalent with AR (%)
4.30.9	900°C	26-31	602.3	635	514	19.5	10.0	13.3
4.31.9	850 ^O C	59-76	591	601	376	6.6	7.2	9.8
4.31.9	875 ⁰ C	40-49	597	604	448	6.3	8.6	11.6
4.31.9	900°C	27-34	598	594	461	7.1	8.9	12.0
4.31.9	925 ⁰ C	18-19	598	576	475	8.6	9.2	12.4
4.33.9	850°C	55-65	598	628	474	9.1	9.2	12.3
4.33.9	875 ⁰ C	39-48	603	633	516	9.3	10.1	. 13.4
4.33.9	900°C	29-34	602	610	514	11.1	10.0	13.4
4.33.9	925 ⁰ C	19-21	602	595	510	14.3	9.9	13.2
5.41.9	900°C	31-39	601	648	524	6.5	9.2	12.4
5.41.9	925 ⁰ C	20-23	603	630	522	7.9	9.2	12.3
5.44.9	875 ^O C	42-48	601	676	556	7.9	9.8	13.1
5.44.9	900°C	33-37	604	664	559	8.8	9.9	13.2

Table 3.2-3
DIFFUSION EXPERIMENT 6-48-9

Diffusion					Meas	surements (No	A/R)			
		Ter	. On	Time (Minutes)	Sheet-R	V _{oc}	$^{\mathrm{I}}$ sc	¹ 500	R _{sh}
Group				N ₂ -Only	O ₂ -Only	Ω/[]	mV	mA	mA	Ω
		-								
	A*	8.5	0	15	5					
	B,*	85	0	25	5					
	С	87	5	10	5	43 (38-56)	601 (579-606)	696 (656-721)	450 (162-575)	(45-125)
	D*	87	5	15	5					
	E	90	0	7	3	32	628 (599 – 628)	700 (685 – 708	557 (510-594	56 (42-100)
13	F	90	0	10	5	24 (23 – 26)	605 (602-607)	689 (681 - 697	572 (523-600)	63 (38 - 179)
	G	92	5	5	2	29 (28 – 30)	605 (603 - 607)	698 (689 - 707)	611 (604-621)	28 (22-36)
	H	92	5	7	3	24 (23–25)	605 (602 – 606)	687 (682 – 665)	606 (592-619)	24 (15-42)
	I	95	0	4	1	22 (19 - 23)	602 (597 - 604)	666 (659 – 673)	574 (610-606)	26 (12-83)
	J	95	0	5	2	19 (17 - 21)	601 (592 - 627)	660 (632 – 668)	518 (569 - 598)	19 (11 - 167)

^{*}Experiment failed due to operator error at diffusion step.

Table 3.2-4
DIFFUSION EXPERIMENT 6-51-9

		Diffusion				surements (No	A/R)	
	Temp.	Time (Minutes)	Sheet-R	V _{oc}	I _{sc}	^I 500	R _{sh}
Group	oC_	N ₂ -Only	O ₂ -Only	Ω/□	mV	mA	mA	Ω
Α	875	25	5	29	608	683	508	75
				(26-34)	(606-611)	(664-706)	(384-565)	(36-119)
• B	875	15	5	38	602	690	470	76
				(34-42)	(590-607)	(666-711)	(391-506)	(41-113)
C*	875	7	3	35	605	710	544	117
			•	(34-37)	(603-607)	(698-719)	(510-572)	(29-185)
D*	900	7	3	52	602	712	446	86
		• •	•	(50-55)	(601-605)	(704-721)	(377-496)	(63-116)
E	900	. 5	2	32	604	698	543	102
				(31-34)	(601-606)	(681-712)	(507-563)	(45-152)
F	900	4	1	57	600	706	419	87
				(53-60)	(597-604)	(689-724)	(259-478)	(22-139)
G	925	5	2	28	604	692	565	84
				(27-29)	(602-605)	(681-702)	(517-590)	(43-132)
Н	925	4	1	34	602	696	517	63
-				(32-35)	(600-604)	(685-713)	(473-546)	(39-94)

^{*}It appears like a mix-up between Groups C and D; might have been interchanged.

cells diffused at different temperatures. The best cells were obtained from wafers diffused at 925°C. The improved sensitivity of run 6.48.9 as compared to previous experiments is attributed to the improvement in shunt resistance.

There is a significant difference between Emulsitone N-250 and Accuspin PX-10 diffusion with respect to times necessary to obtain similar sheet resistances. This is believed to result from the phosphorous surface concentration of wafers diffused with PX-10 being considerably larger than that obtained by using N-250. This could have negative effects on performance due to larger dead layer effects and might affect contact adhesion.

3.3 BACK SURFACE FIELD

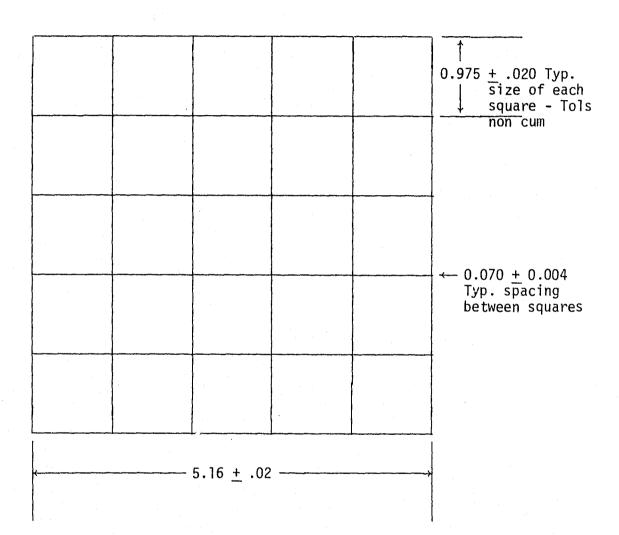
3.3.1 Cell Bowing

The P+ back surface field process with an aluminum back contact is presently producing very good cells. The voltage is in the range of 610 to 620 mV, but there is one potential problem. The aluminum produces a strain in the cell due to the thermal expansion coefficient difference between silicon and aluminum. The strain causes the wafer to bow, which may create problems with automatic handling equipment. A proposed solution to this bowing problem is to allow streets of bare silicon between blocks of aluminum, Figure 3.3-1. Two questions need to be answered concerning this patterned aluminum back. First, how effective is the pattern in reducing the bowing. Second, does the pattern reduce the effectiveness of the back surface field.

To measure the effect of bowing, 2.12×2.12 inch wafers were thinned by etching to 5 mils and printed with both a normal full back contact and the new patterned back contact, run 4.23.9. Both

Figure 3.3-1
Pattern for Aluminum Back

to Reduce Bowing Effects



DIMENSIONS ARE IN CENTIMETERS TOLERANCES: .XXX = + .02 Back Contact Pattern P+ (Screen Printing)

PART NO. NM 516-P-070

Note: Squares are areas of open screen

sets of wafers had a radius of curvature of 7.5 cm after firing. The cylinder defined by the curvature was parallel to the support rods of the sintering boat, Figure 3.3-2. After the wafers were dipped in a dilute solution of hydrofluoric acid and the unconsolidated aluminum was removed by brushing, the wafers had a radius of curvature of 16.5 and 79.5 cm for the full back and pattern back, respectively, indicating that the pattern is indeed effective in reducing the bowing effects.

The second experiment, run 5.35.9, was designed to determine the effect of the pattern back on cell electrical performance. The wafers were processed in accordance with the baseline process except the wafers were laser scribed prior to front silver metallization and no AR coating was applied. The open circuit voltage was the same for both back contact patterns, and the efficiencies were 9.0% (=12.1% with AR coating) and 8.5% (=11.4% with AR coating) for the pattern back and full back, respectively. Both of these sets of cells had low output due to shunting problems.

In order to obtain a larger data base on the pattern back surface field, three separate runs were processed, 5.43.9A, B, and C, by three different technicians. These runs were processed the same as those of run 5.35.9. The cell characteristics of all three runs were practically the same, very similar to the results of run 5.35.9. The results are summarized in Table 3.3-1.

In comparing the shunt resistance from run 5.46.9 reported earlier in this report, and all other runs reported, it is evident that the 10 ohm-cm material from Wacker produces cells with superior shunt resistance. This may be due to the low impurity level in 10 ohm-cm material. A larger data base must be established before an accurate conclusion can be drawn.

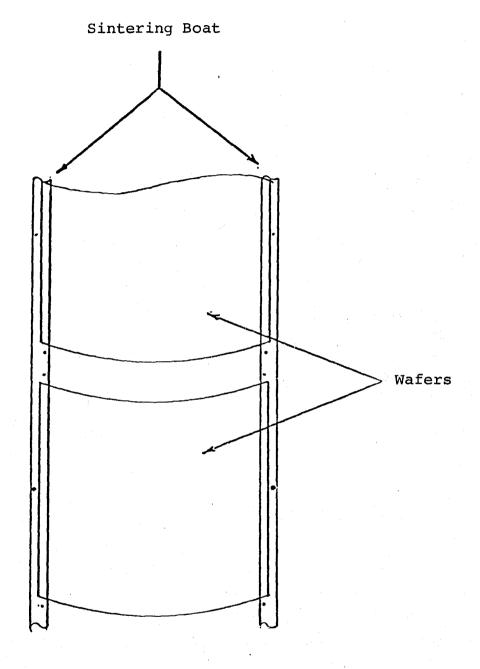


Figure 3.3-2
RELATIONSHIP OF CELL BENDING TO SINTERING BOAT CONFIGURATION

Table 3.3-1
BACK SURFACE FIELD

Average Values

Run #	p+ Back	Sheet ρ (Ω/\Box)	Voc (mV)	I sc (mA)	^I 500 (mA)	R _{sh}	(%)	Equiv. n with AR (%)
5.25.9	Pattern	32-36	604	650	525	6.4	9.0	12.1
5.35.9	Ful1	32-40	603	648	498	4.9	8.6	11.5
5.35.9	Full	28-40	604	651	487	5.8	8.5	11.3
5.43.9A	Pattern	33.3	602	659	512	7.3	9.0	12.1
5.43.9B	Pattern	33.6	602	669	505	6.9	8.8	11.9
5.43.9C	Pattern	32.6	603	664	516	4.7	9.1	12.2

As a further qualification of the pattern back 10 Ω -cm and 2 Ω -cm material was prepared in accordance with our baseline process except the junction was chemically cleaned and was not AR coated, (Run 6.50.9). The results indicate that the power loss due to series resistance is larger in the 10 Ω -cm material, but the power loss due to shunt resistance is smaller in the 10 Ω -cm material (Table 3.3-2).

3.3.2 Mesh Screen Sizing

In order to determine the effects of screen mesh size on the printing of the aluminum paste, 2-inch round wafers were processed in accordance with Table 2.1-1 except for chemically etching the edges of the cells. Run 4.26.9 (Table 3.3-3) was divided into two groups where the aluminum paste was printed with 165 and 105 mesh screen. The cells printed with the 165 mesh screen had a slightly higher Voc and current at 500 mV. The difference between the two screening masks does not appear to be significant.

3.4 CLEANING PRIOR TO FRONT METALLIZATION

Major shunt resistance problems have plagued Spectrolab's cell fabrication since the beginning of the year. The problem has been traced to the front metallization and/or application.

Surface condition prior to front metallization appears to be a factor in cell performance. It was observed that processed wafers which have had a long period of storage prior to front metallization have lower shunt resistance. This observation led to an experiment in which wafers were prepared in accordance with our baseline process except the junction was chemically cleaned, wafers were etched in 10% solution of Hydrofluoric acid for 30 seconds immediately prior to front metallization and not AR coated (Run 6.47.9). The shunt resistance was 3 times as high and the efficiency was 9.6% (=12.8% with AR coating), 1.3% higher than

TABLE 3.3-2
RUN 6.50.9

Performance of Cells with Patterned Aluminum Backs

Base resistivity		Ave	erage Valu	ıes
ohm-cm	V _{OC} mV	I _{sc}	^I 500 <u>mA</u>	Rsh ohms
10 ohm-cm	596	707	580	64.9
2 ohm-cm	604	686	610	28.7

TABLE 3.3-3

RUN 4.26.9

Effect of Screen Mesh Size on Back Surface Field

No AR Coating

2.12" Round Cell

			Ave	erage	
	**************************************	V (mV)	I _{SC}	^I 500 (mA)	R _{sh} (ohms)
165 Mesh		609 ± 3	513	446	11.9
105 Mesh		606 ± 3	512	432	11.7

the wafers not treated with HF. These results indicate that an HF surface treatment prior to front metallization is beneficial. The HF surface treatment is probably removing excess aluminum particles as well as the oxide on the front surface. If this treatment is removing excess aluminum particles, HCl will work just as well.

In run 6.49.9 the surface was treated with HF and/or HCl for a total time of 30, 60 and 120 seconds, Table 3.4-1. The most consistent results were from the group which had an HCl and HF gave favorable results also. These results support the hypothesis that aluminum particles remain on the front surface after the back cleaning step. They should be removed with HCl and/or HF.

The original surface cleaning step prior to front metallization, outlined in Table 3.4-2, was intended to remove any ${\rm AlF}_3$ and ${\rm AlCl}_3$ material remaining after the HCl and/or HF surface treatment. In run 6.52.9 wafers were cleaned to various stages of this cleaning step in an attempt to determine the beneficial and detrimental stages and also to reduce the number of stages. The average value for ${\rm V_{oc}}$, ${\rm I_{sc}}$, ${\rm I_{load}}$ (500 mV) and shunt resistance is tabulated in Table 3.4-3.

The acetic acid and acetone were beneficial to cell performance. The first hot D.I. water rinse appears detrimental. The alcohol and second hot D.I. water soak may not be necessary.

3.5 PRINGED SILVER FRONT CONTACT

The series resistance of the current cell design fabricated with screen printed front metal was evaluated. The front collector pattern was found to be a major contributor to the series resistance. The measured series resistance was in the range of 80 to $100~\text{m}\Omega$. The series resistance was calculated to be 90 m Ω as

at main

Table 3.4-1

Run 6.49.9

Acid Treatment After Aluminum Brushing and Before Printing Front Contact

Treatment		v _{oc}	sc	<u> 1500</u>	Rsh	
HC1	30	Sec.	598	617	469	12.6
HCl	60	Sec.	602	621	510	18.7
HCl	120	Sec.	606	655	580	33.4
HF	30	Sec.	604	639	551	32.7
HF	60	Sec.	603	626	535	34.7
HF	120	Sec.	605	650	576	49.0
HC1 HF		Sec. Sec.	606	650	582	49.5
HCl HF	30 30	Sec. Sec.	604	642	564	22.7
HCl HF	60 60	Sec. Sec.	606	661	590	44.8

Table 3.4-2

CLEANING STEP

Sleaning Treatment Prior to Printing Front Metal

Influence on Cell Performance

- Beneficial 1) 50% Acetic Acid, 1 minute (RT)
- Detrimental 2) Rinse in hot D.I. water, 30 sec. (75-90%)
- Beneficial 3) Rinse in acetone, 30 sec. (RT)
- Beneficial 4) Soak in acetone, 2 min. (RT)
- Unknown 5) Soak in alcohol, 2 min. (RT)
- Unknown 6) Soak in hot D.I. water, 2 min (75-90°C)
 - 7) Rinse in cold D.I. water and spin dry

Table 3.4-3

Run 6.52.9

Performance of Cells with Various Cleaning
Treatment Prior to Printing Front Metal

Stages Included in Cleaning Step	Voc	Isc	I ₅₀₀	R _{sh}
7	603	676	409	7.8
1 + 7	609	694	510	17.6
1 + 2 + 7	606	698	419	10.4
1 + 2 + 3 + 7	608	694	485	13.5
1 + 2 + 3 + 4 + 7	611	702	553	25.6
1 + 2 + 3 + 4 + 5 + 7	610	701	542	26.0
1 + 2 + 3 + 4 + 5 + 6 + 7	610	702	555	24.9

^{*} Defined in Table 3.4.2

summarized in Table 3.5-1. The detailed calculation is given in Appendix 1. The major contribution is that of the ohmic collector bar. In order to verify these results, the center ohmic collector of a cell was coated with solder. The change in the I-V characteristics (Figure 3.5-1) indicates a 25 m Ω reduction in series resistance. Experiment 6.51.9 (Table 3.5-2) further verified these results. The present front ohmic collector could be redesigned to be more effective.

As a part of this evaluation the conductivity of the front contact metal was examined. Test patterns were screened onto 50 ohm-cm 2" silicon wafers to provide suitable lines on which to perform measurements (see Figure 3.5-2). The effective line length of the pattern is 72.90 cm and the width and height vary with the paste used. Widths were measured by Tally-Surf and optical methods. The resistance of the printed contact line was measured with a General Radio Digi-Bridge meter which has a resolution of 1 milliohm. The resistance of each half of the pattern was measured in addition to the entire pattern to guard against isolated gaps or pinched down regions. Measurements of all lines in one pattern revealed a maximum of 4% variation in fourteen 1.95 cm long lines which is indicative of uniformity within a pattern.

Three different silver conductive thick film pastes were tested including the currently used Thick Film Systems 3347 + 2% Transene N-Diffusol. The resistance, half pattern resistance and line width are measured values which were used to calculate the resistivity and line thickness. These values are presented in Table 3.5-3. The cross-sectional area necessary for the resistivity calculation was determined by gravimetric integration of the Tally-Surf curves for each paste. The effective line thickness was then calculated from the line length, based on resistivity.

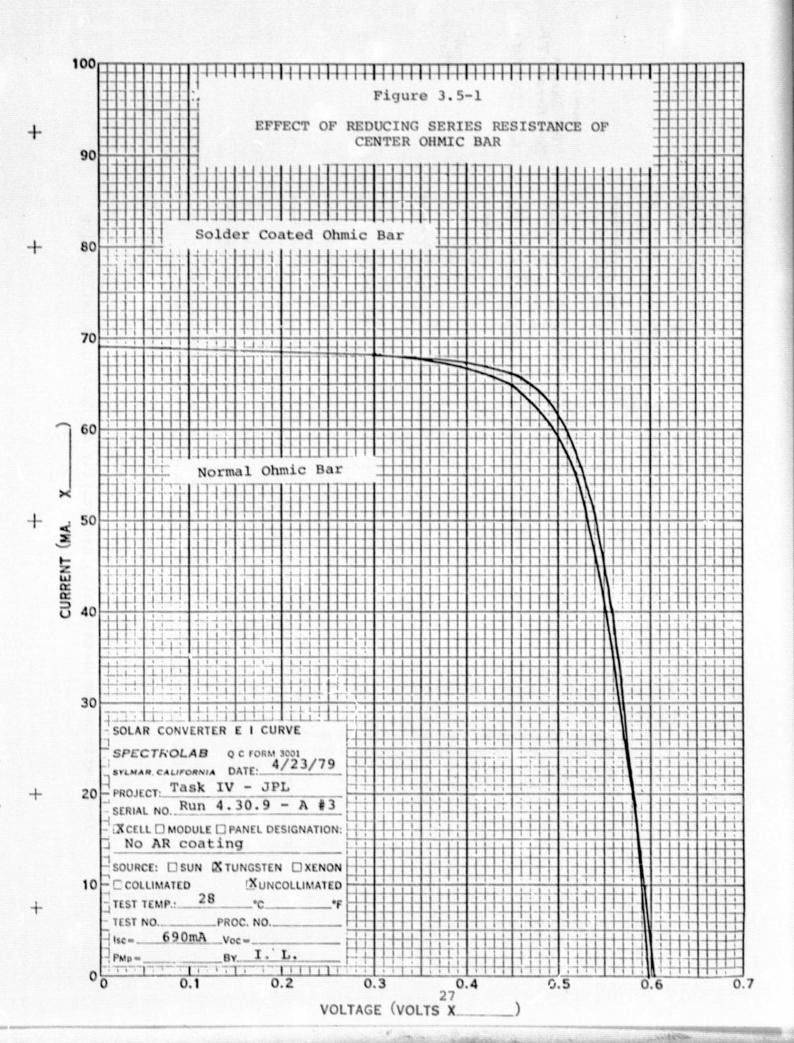
Table 3.5-1
Calculated Contributions to Cell
Series Resistance

Component	Resistance
Base Region	3.4 $m\Omega$
Diffused Layer	14.9 $m\Omega$
Gridlines	$7.0~m\Omega$
Collector Bar	64.8 mΩ
Total	90.1 $m\Omega$

Table 3.5-2 EXPERIMENT 6.51.9 AVERAGE VALUES

Effect of Solder Coating Ohmic Collector Bar on Cell Performance

BEF	ORE SOLDER C	N OHMIC	AFTER	SOLDER ON O	HMIC
V _{OC}	I _{sc}	^I 500 mA	V _{OC} mV	I _{sc}	^I 500 mA
604	702	507	604	706	565
(599-611)	(688-719)	(339-590)	(600-610)	(669-727)	(388-638)



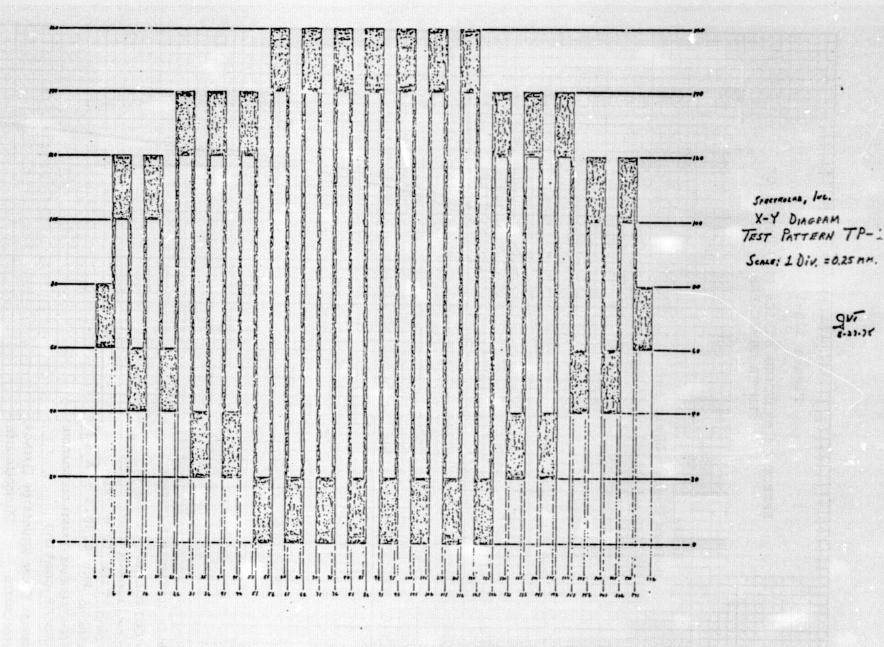


Figure 3.5-2
Test Pattern for Determining Resistivity of Contact Metallization

Table 3.5-3
RESISTIVITY OF COMMERCIAL SILVER PASTES

	Resistance				Cross-		O
Thick Film Paste	Full Pattern (2)	Half Pattern (Ω)	Line Width (mil)	Resistivity (μΩ-cm)	Sectional Area (mil ²)	Line Thickness (mil)	ρ PAg PAg=1.6μΩ-cm
Dupont	9.48	4.83/4.77	14.0	2.90	3.46	.25	1.8
Electro Sci- ence Lab Ag590	7.935	4.00/4.06	10.1	5.07	7.23	.71	3.2
Thick Film Systems 3347+2% N-Diffusol							
Sample 1	5.96	3.03/3.03	10.0	4.20	7.96	.80	2.6
Sample 2	7.48	3.86/3.73	10.0	4.62	6.97	.70	2.9

All samples fi-ed at 700°C for 40 seconds in 20% O_2 , 80% N_2

The resistance of the TFS-3347 + 2% N-Diffusol paste was the lowest although the resistivity ($\rho_{\rm TFS}=2.75\rho$ bulk silver) is higher than the Dupont 7095. The Dupont paste had the lowest resistivity ($\rho_{\rm Dupont}=1.8\rho$ bulk silver), however, less material was deposited and it flowed more, resulting in thinner, wider gridlines of smaller cross-sectional area. The ESL AG590 paste had a slightly higher resistance and resistivity than the TFS paste.

To reduce the series resistance a screen with a 2 mil emulsion was procured and evaluated. This screen indeed reduced the series resistance from about 90 to 60 milli-ohms for the 1 and 2 mil emulsion screen, respectively. However the screen with 2 mil emulsion has a greater tendency to clog the 6 mil gridlines. This results in broken printed gridlines and higher series resistance. An improved method for producing cells with low series resistance would be to apply the gridlines and center ohmic collector in two separate operations, with the introduction of a cost penalty for the additional screen printing operation.

3.6 JUNCTION ISOLATION

The Spectrolab baseline process includes laser scribe for junction cleanup. This may be accomplished by scribing the back side then breaking or scribing through the junction from the front side.

To determine the effects of laser scribing on the cell's characteristics, wafers were processed in accordance with our standard process, except the wafers were divided into two groups prior to junction cleaning. The first group was saw cut and chemically etched and the second was laser scribed from the back and cleaned, run 4.29.9. The results of these two groups, Table 3.6-1, were very similar indicating that laser scribing is an effective method of junction removal.

To confirm the results of run 4.29.9, we ran a similar group of wafers, run 4.32.9, Table 3.6-2. (Eight cells were saw cut and chemically etched as a control and the remaining 25 cells were laser scribed.) The results were very encouraging; the saw cut and chemically etched cells had an average efficiency of 9.2% (12.4% with AR coating) for 6 out of 9 cells. Laser scribed cells had an average efficiency of 9.7% (12.9% with AR coating) for 25 out 25 cells. The laser scribed cells probably had a larger yield due to decreased cell handling.

These initial findings suggest junction clean-up though laser scribing and breaking is equal to or better than saw cutting and edge etch treatment. However, there are some problems associated with this process. If we begin with square wafers, laser scribing through the Al (p+) layer produces silicon waste. A minimum of 50 mils may be successfully cleaved from each edge. Starting with a 4" x 4" wafer, a minimum 5% loss of material is realized in laser scribing and cleaving. Junction isolation, by scribing a shallow street along the front edge of a finished cell, would eliminate damage and waste. The shallow street may be laser scribed as close as 10 mils to the edge of the cell decreasing the active area of a 4" x 4" cell by 1%.

Junction isolation by laser scribing from the front will need development. It is believed a low power output (1-5 watts), laser beam is needed to scribe a shallow street that is free of silicon remelt material which may cause current leakage. In the present resonator mode, TEM₀₁, 10-15 watts average power are delivered in a hollow cylindrically-shaped beam. Looked at in a cross section the beam strikes the substrate at two points of greatest intensity. Depending upon laser pulse frequency, chuck speed, and laser current input, silicon remelt material may build up. These variables control laser drilled hole overlap, laser kerf width, and laser scribe depth. The interaction of these variables can be described by the

Table 3.6-1
Run 4.29.9

Preliminary Comparison of Saw Cutting with Chemical Etch and Laser Scribing

No AR Coating (2.0 x 2.0")

	Averages of 8					
	V (mV)	I sc (mA)	^I 500 (mA)	R _s		
Saw Cut	601	674	491	7.65		
Laser Scribe	601	644	491	5.72		

Table 3.6-2

Run 4.32.9

COMPARISON OF SAW CUTTING AND CHEMICAL ETCH AND LASER SCRIBING

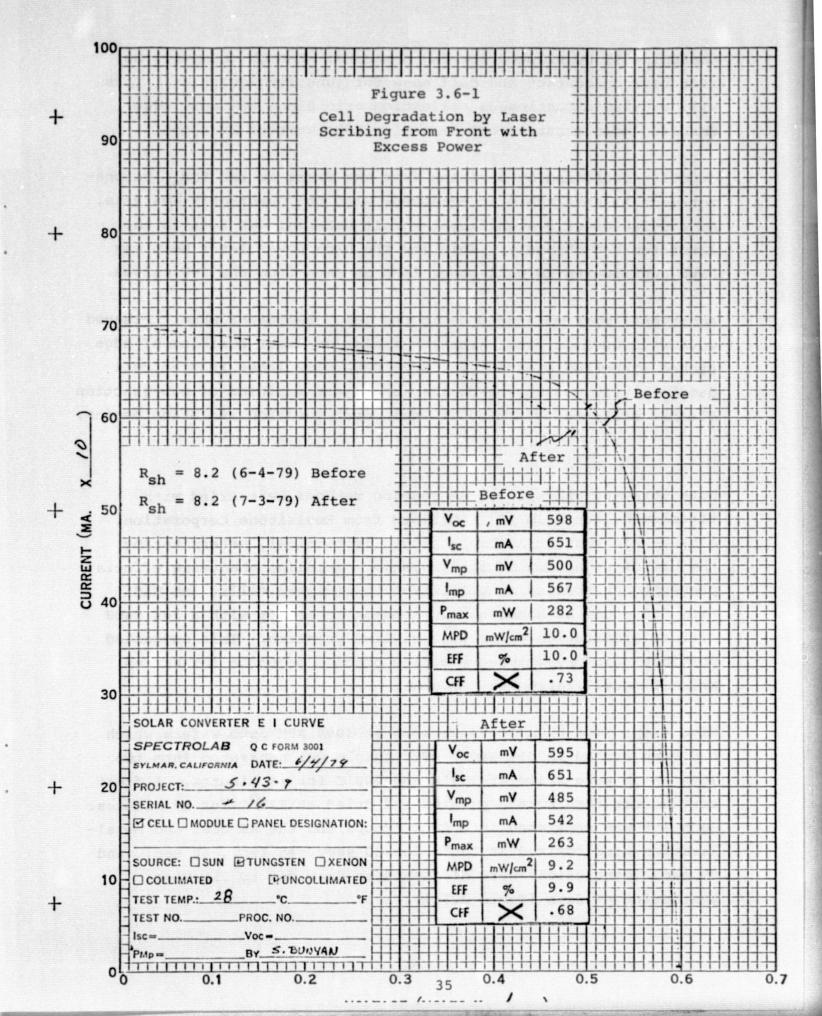
No AR Coating (2.1" x 2.1")

	V OC (mV)	Isc (mA)	^I 500 (mA)	R _{sh}
Saw Cut Average	602	644	498	13.1
Laser Scribe Average	603	670	551	11.7

Q-factor. The Q-factor is equal to the product of kerf width (mils) and pulse frequency (KHZ) divided by chuck speed (IPS). It has been stated by the laser scribe manufacturer, Quantronix Corporation, that material is ejected from the kerf at an angle of 45° to the substrate surface with little or no residue remaining in the kerf at a Q-factor of 3. At Q-factors greater than 3, material is ejected at increasingly lower angles to the substrate surface and some material is trapped as a slag residue. At Q-factors less than 3, laser drilled holes overlap insufficiently to form a continuous kerf. At a Q-factor of 3 in the TEM₀₁ mode, junction damage may result from the high power. In the TEM₀₀ resonator mode a solid cylindrical line beam strikes the substrate at 1-5 watts. A low power, point-focused beam may be allow complete evacuation of material with no junction damage.

As part of an initial evaluation of the suitability of front side laser scribing for junction isolation, twenty 2.1 x 2.1" cells were fabricated. Shunt resistance measurements and I-V curves were taken prior to laser scribing. Chuck speed varied from 8 to 10 inches per second, laser current input was set at 34 amps and pulse frequency was set to ensure a Q-factor of 3 using TEM_{01} . The cells were then laser scribed and all measurements retaken.

Short circuit current (I_{sc}) measurements did not decrease, and open circuit voltage measurements decreased slightly. Microscopic inspection of the laser scribed grooves showed signficant remelt material. Cell degradation was evident from the shapes of the I-V curves (Figure 3.6-1). This degradation appears to be associated with a decreased shunt resistance. The shunt resistance measured by dark current techniques did not change. This would be consistent with shunting at the laser scribe line which would be masked in the dark current measurement by spreading resistance between the grid fingers and scribe lines. An experiment is planned to test this. At the edge of our present grid pattern a 30 mil wide



contact will be printed forming a square. Enough room will be left between contact and cell edge for junction isolation. This will provide a continuous collection grid along the cell edge enabling more accurate determination edge current leakage.

Junction isolation by scribing from the front in the TEM₀₁ resonator mode is unsuitable in agreement with the Quantronix analysis. At a Q-factor of 3 significant remelt material was seen in the laser scribed channels. This and the high power laser beam may have contributed to cell power loss as seen from the I-V curves.

Additional work will be done in the TEM₀₀ Resonator mode. Planned work will include front junction isolation laser scribing of edge etched (junction cleaned) cells to determine laser induced cell damage at various scribe depths, and laser scribing of non-junction cleaned cells to determine at what depth junction isolation begins.

3.7 AR Coating

Both spray-on and spin-on AR coating methods were tried with titanium-Silica Film "C" obtained from Emulsitone Corporation. A hand-held Paasche Airbrush proved impractical, necessitating the use of an automatic spray system. Gridline shadowing effects prevented uniform spin application to finished cells, but TiSi Film "C" could be homogenously spun-on to wafers with a 30% NaOH surface preparation prior to gridline printing. This suggested possible spin-dry-print-dry-cofire process sequence for screen printed metallization and AR coat.

Five drops TiSi Film "C" were spun at 3000 RPM onto wafers which had been etched in 30% NaOH. The sample was separated into two lots which were dried at 150°C and 200°C for 15 minutes. A front contact was then screen-printed and dried at 125°C for 15 minutes. Each lot was separated into four groups, and the AR coat and metallization were cofired at 700°C for 30 sec., 45 sec., 60 sec., and 75 sec. Conclusions were difficult to draw due to the wide scattering of data (Table 3.7-1).

Table 3.7-1

EVALUATION OF SPIN-ON SUITABILITY OF TITANIUM SILICAFILM "C"

Run 5.37.9

			•			
			V _{OC} (mV)	Isc (mA)	^I 500 (mA)	R _{sh}
Contr	01					
		Average	603	489	439	22.8
150°C	Bake Sec.	Sinter	607	618	331	33.8
30	sec.	Sincer	607 608 613 611	614 618 614 629	356 392 450 383	16.0 80.7 43.9 46.3
45			606 606	623 606	413 335	22.1 12.5
60		·	605 604	622 621	378 399	18.4 21.6
75		,	600 598	613 606	179 220	17.4 18.0
200 ^O C	Bake					
30	Sec.	Sinter	609 611 606 601 609	623 607 611 609 620	409 441 393 397 478	29.6 62.5 22.3 10.4 25.8
45			603 598	623 611	315 213	14.2 14.4
60			607 604	628 632	518 352	34.3 19.5
75			606 600	626 591	494 286	23.4 36.0

A second experiment was devised varying the drying time at a constant temperature and spin velocities around values used in the previous experiment. The firing schedule was 30 seconds at 700° C. The short circuit current (I_{sc}) increased with decreasing spin velocity, peaking at the slowest spin velocity. However, output was not similarly dependent on spin velocity. Cell characteristics did not vary with drying time. Results are summarized in Table 3.7-2. This process configuration is not acceptable because of the high series resistance.

Spin-on difficulties prompted the investigation of spray-on AR sources with an Advanced Concepts spray system using equipment at Sensor Technology, Inc. The Advanced Concepts spray system consists of a spray chamber followed by a convection heating oven and infrared furnace. A reciprocating spray head moving back and forth across the sample deposits an atomized mist. Spray parameters include conveyor velocity, reciprocator velocity, atomization pressure and the flow rate of the liquid material being applied.

Attention was also shifted to a titanium isopropoxide AR solution developed by RCA, shown by them to have the capability of 35% efficiency enhancement (slightly better than they observed with TiSi film "C"). After much experimentation a uniform blue-violet AR coat was applied to wafers etched with 30% NaOH.

Square cells oriented with gridlines parallel to and center ohmic perpendicular to the reciprocator motion were coated and dried with the results summarized in Table 3.7-3. The surface appeared speckled with light colored strips 1/16" wide running the length of the trailing edge of each gridline.

Effect of Drying Time and Spin Rate of AR Coating
Application - Cofiring of AR Coat and
Front Metal Contact

Table 3.7-2

	V _{OC} (mV)	Isc (mA)	^I 500 (mA)	R _{sh}	$\frac{R_{ser}}{(m\Omega)}$
Control	608	535	479	19.1	95
1A	612	629	408	17.3	277
1B	614	631	432	27.2	242
1C	615	618	502	21.0	161
1D	614	607	437	25.0	242
lE	614	602	469	22.9	193
2A	612	634	418	14.5	222
2B	616	630	508	17.2	147
2C	616	622	576	23.7	132
2D	612,	606	435	21.5	101
2E	615	601	503	35.7	89
3A	614	629	455	21.1	233
3B	615	624	482	15.0	147
3C	614	617	497	18.8	147
3D	611	601	471	16.8	161
3E	614	601	502	11.6	112

^{1 - 200°, 10} min. dry

^{2 - 200°, 20} min. dry

^{3 - 200°, 50} min. dry

A - 2000 RPM spin

B - 2500 RPM spin

C - 3000 RPM spin

D - 3500 RPM spin

E - 4000 RPM spin

Table 3.7-3

INITIAL EVALUATION OF EFFICACY OF SPRAYED ON TITANIUM ISO-PROPOXIDE AR COATING

	Voc	I _{sc}	^I 500
Average Before AR	603	670	492 (2.1" x 2.1" sq. cells)
Average After AR	609	846	689

Average Increase: I_{SC} 26%, high of 31%

Average Increase: I_{500} 25%, high of 31%

Spray parameters were as follows:

source flow rate	10 mil/min.
atomization pressure	30-35 psi
reciprocator velocity	90 CPM
conveyor velocity	2 ft./min.
reciprocator height from substrate	6 in.
orifice size	12 mil

These wafers were processed in an IR furnace peaking at 250°C followed by a 60-90 sec. 200°C hot plate bake-out. A three step bake-out of 70°, 200°, and 400°C - 30 sec. each is recommended by RCA and will be investigated. Other planned work includes further optimization of spray parameters and bak-out procedure to eliminate coating nonuniformities.

3.8 MODULE ASSEMBLY

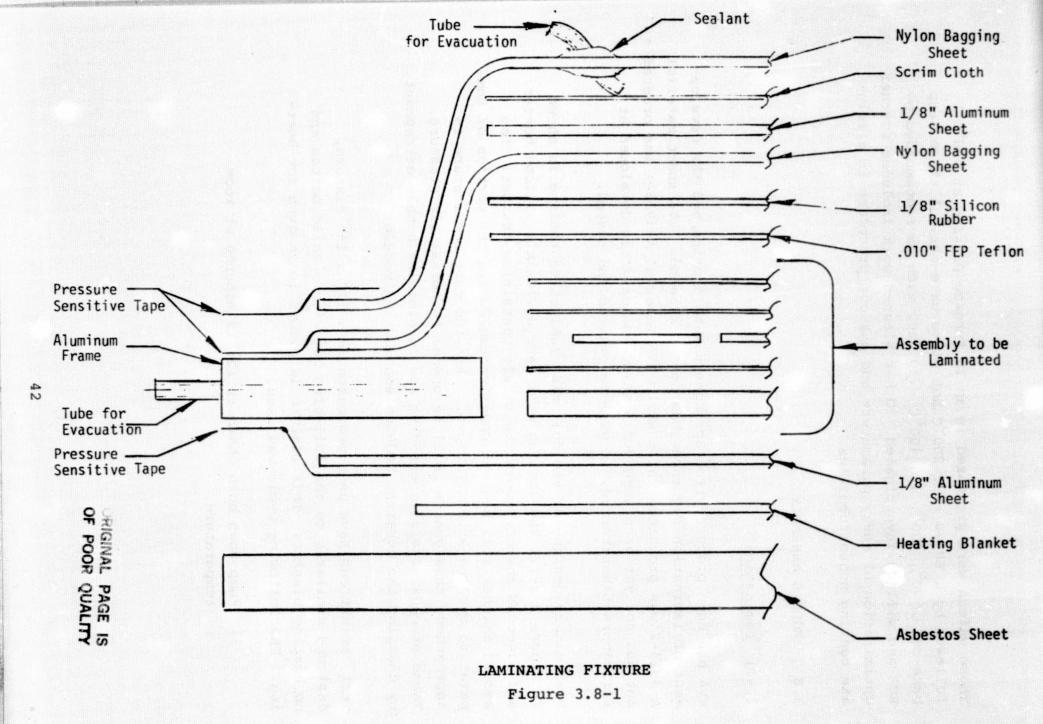
3.8.1 Lamination

EVA has been procured from Springborn Laboratories, and the development of lamination sequences has been initiated. EVA sheet material A-8914-2 was procured, while white EVA material A-8916-A was ordered but has not yet been received. As new material is developed at Springborn Laboratories, it will be ordered and tested.

Preliminary design for the full size lamination tooling is shown in Figure 3.8-1. The tooling will have a flexible silicon heater, and a second chamber above the module-containing chamber. The second chamber will be kept under vacuum during the portion of temperature cycling when EVA flows. When the cure temperature is approached, this chamber will be opened to normal air pressure. These procedures are expected to aid in avoiding bubble entrapment by changing the apparent modulus seen by the module.

Test laminations have been processed in a 12" x 15" fixture, designed similarly to the full-size but with a solid bottom and no heating blanket. This fixture is placed in an oven for heating. The following cycle was used:

1) Pump down both chambers for 15 minutes at room temperature;



- 2) Place assembly in oven at 100°C for 15 minutes;
- 3) Remove vacuum from upper chamber;
- 4) Heat oven to 150°C;
- 5) Let sit at 150°C for 15 minutes;
- 6) Remove.

This cycle produced flawless test samples and will be used for larger verification modules.

3.8.2 Interconnections

Interconnect ribbon has been procured. Cell-to-cell interconnects will be 1" lengths of 2 mil x 0.10 inch copper ribbon. The ribbon is OFHC copper with 1/2 mil solder plating that has been fused. Bus bar material is 3 mil x 0.40 inch copper ribbon, OFHC, 1/2 mil plate, fused. Using the wider ribbon as a bus bar at both ends of the panel (connected to ten 20-cell strings) with termination at the center, the power due to resistance loss in interconnects is approximately 0.3 watts. See Appendix 2 for calculations. These calculations are extremely conservative, using resistance at 75°C, power at room temperature and not including any conductance for the solder plate.

A fixture has been built to connect cells into strings. Cells which have been front tabbed are used. The fixture consists of a 3" x 3" heating block with vacuum hold-down attached to a non-heated block 3" x 24" through a thin teflon block. The teflon block is machined such that there is a .050" spacing between a cell on the heated and unheated block. The small block is heated to 150°C. An ultrasonic soldering iron is used to first put a tin/zinc solder pad on the cell back. This constitutes a shift of this process step from the cell processing sequence to the module assembly sequence. Next, the interconnect (from the adjacent cell

positioned on the unheated block) is ultrasonically soldered to the pad. This creates a two-cell string which is slid to one side so another cell may be attached. Longer strings are thus created with great accuracy of intercell spacing.

Pull tests have been completed on cells interconnected in this manner. Back interconnect strengths are shown in Table 3.8-1. 90° pull test failures all exceeded 700 grams; and 45° pull test failure strengths were greater than 1400 grams, the maximum load our test fixtures can apply. Failures that occurred below 1000 grams were all due to silicon fracture. Front interconnects were tested with the 90° pull test (Table 3.8-2). A correlation of the strength of the joint with the amount of time between HF etch and front contact printing was found. If the cells are printed within 24 hours, pull strengths greater than 650 grams are found. As the amount of time between HF etch and printing is increased, the pull strengths lessen. If the time is two weeks, the front contact shows no adhesion to the cell. In all front contact pull tests the failure mode is the silver contact separating from the silicon.

Table 3.8-1
BACK INTERCONNECT PULL RESULTS

90° Pull

Cell #	Load at Failure (Grams)	Failure Mode
. 1	1000	Peel
2	1100	Peel
3	700	Cell Fracture
4	750	Cell Fracture
. 5	1150	Cell Fracture
6	1400	Cell Fracture
7	>1400	None
8	750	Cell Fracture
9	1000	Peel

45° Pull

Cell #	Load at Failure (Grams)	Failure Mode
1	>1400	None
2	>1400	None
3	>1400	None
4	>1400	None
5	>1400	None
6	>1400	None
7	>1400	None
8	>1400	None
9	>1400	None

Table 3.8-2 FRONT INTERCONNECT PULL RESULTS 90° pull, solder press used

Cell #	Failure Load	
1	71 0 g	
2	680	Printed 24 hours
3	870	after HF etch
4	800	
5	590	
6	1030	Printed 1 week
7	570	after HF etch
8	460	
9	5	
10	5	Printed 3 weeks
11	5	after HF etch
12	5	

4.0 CONCLUSIONS

The following conclusions have been reached durint this period:

- 1) Evaluation of (110) wafers by our normal process sequence Table
 2. 0-1 indicates that the (110) surface etches at twice
 the rate of (100) surface and the (110) surface appears partially textured. Thus, this surface preparation would produce
 an irregular surface when used on EFG ribbons or polycrystalline wafers which have many surface orientation.
- 2) The junction formation with PX-10 emitter source produces acceptable cells when diffused at 900 + 25°C.
- 3) The pattern P+ aluminum back contact reduces bowing of wafer with no apparent degradation of cell's performance.
- 4) A two mil emulsion front silver grid screen is effective in reducing series resistance. Printing 6 mil gridlines through a two mil emulsion creates clogging problems which may preclude its use for large scale production. The gridlines and center ohmic collector could be applied in separate steps in order to produce narrow gridlines and a center ohmic with large current capacity.
- 5) Preliminary evaluation of spray-on titanium isopropoxide with the Advanced Concept Spray system have shown good results, efficiency increase of up to 31%. Optimization and evaluation of the source and the spray system cannot be properly obtained until a greater familiarity of the controlling parameters are obtained.
- 6) Junction cleanup by laser scribing (through the back P+ layer) followed by cleaving causes no cell degradation.

7) Laminations of modules using Springborn A-8914-2 EVA have been successful on 12" x 15" modules. Interconnect material has been procured and performs satisfactorily.

5.0 RECOMMENDATIONS

Application of the tin pad to the aluminum back should be moved from the cell process sequence to the module assembly sequence.

6.0 NEW TECHNOLOGY

There was no new technology reported during the period.

APPENDIX 1

SERIES RESISTANCE CALCULATIONS FOR FRONT OHMIC

- 1) Assume 15% efficient cell.
- 2) Assume peak power point at 500 mV therefore we will have an average current density of 30 mA/cm², which includes shadowed areas.

To determine the series resistance we will first calculate the drop in voltage (Dv) due to series resistance.

$$AV = IR \tag{1}$$

Assume:

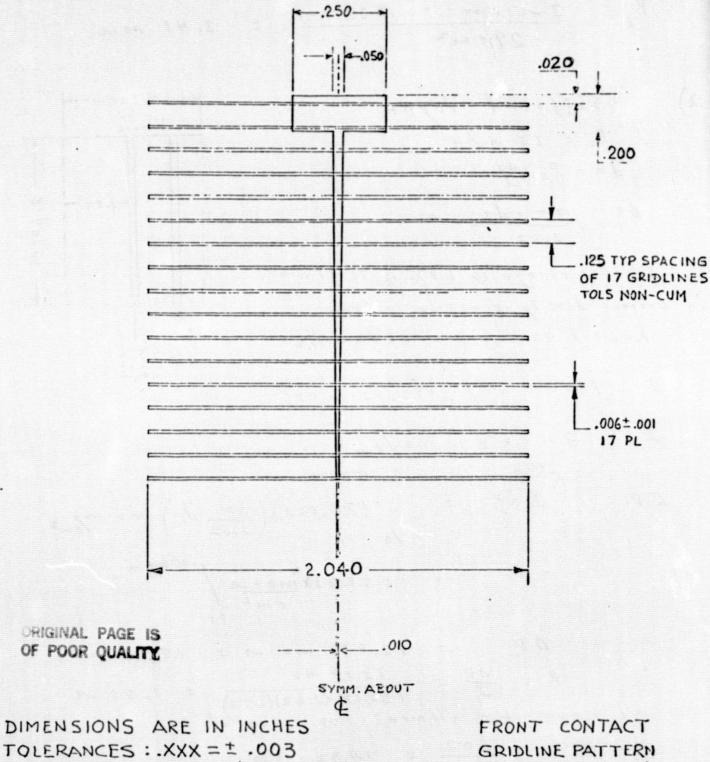
- #1) The 13 mill base material of 3 Ω -cm
- #2) Diffused surface layer 35 Ω/\Box
- #3) Gridlines, that are 6 mils wide and .7 mil thick and a conductivity of 1/3 that of bulk silver
- #4) Center ohmic of .7 mil thick and a width of 10 mils to 50 mils

The total resistance will be the sum:

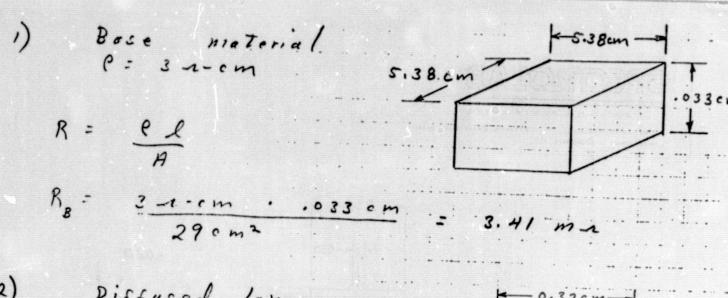
$$R_T = R_E + R_D + R_G + R_{oh}$$

a subsidiary of Hughes Aircraft Co.

1300 GLADSTONE AVE. . SYLMAR, CAUFORNIA SIME TELEPHONE (213) MS-4611



PART NO. 6303-08 GRIDLINE PATTERN (SCREEN PRINTING)



2) Disfused layer
$$P_{s} = 35 n/B$$

$$dR = P_{s} \frac{dx}{dx}$$

$$dR = \frac{35 \cdot dx}{2.62}$$

Silver coverage is 6.9% of total orea

. Current density of active silicon is

1.069 x 30 ma/cm² = 32.07 ma/cm².

$$I = \frac{94.02 \times m_{9}/cm}{.152}$$

$$I = \int_{0}^{.152} dR = \int_{0}^{.152 cm} (84.02x) \left(\frac{35}{2.62}dx\right) \frac{dx}{m_{9}.m_{1}} \frac{dx}{cm^{2}}$$

$$= 561.23x \frac{2}{m_{1}a...} \frac{1}{cm^{2}} \frac{1}{cm^{2}}$$

$$R = \frac{\Delta V}{T} = \frac{12.97 \text{ ma} \cdot n}{(32.07)(2.62)(.152)} = 1.02 \text{ n}$$

$$W \in have 68 elements in parallel$$

$$R_{T} = \frac{1.02}{1.02} = 14.02 \text{ m}$$

 $\frac{1.02}{68} = 14.93 \text{ m} \cdot 1$

OF POOR QUALITY

3)
$$G : d lines$$

$$\begin{cases}
\frac{(l_{Deth})}{sl_{ver}} = 3 & \frac{(l_{ver})(l_{ver})}{sl_{ver}} = 3 & \frac{(l_{ver})(l_{ver})}{sl_{ver}} = 4.77 \times 10^{-6} \text{ a-cm} & \frac{1}{0.0520} = \frac{1}{0.0520} \\
dR = \frac{(l_{ver})}{l_{ver}} = \frac{4.77 \times 10^{-6} d_{ver}}{l_{ver}} = 0.302 \text{ cm} \\
I = (32.07 \text{ mo/cm}^2)(.29 \text{ cm}) I = 2.55 \text{ cm}$$

$$I = (32.07 \text{ mo/cm}^2)(.29 \text{ cm}) I = \frac{2.55 \text{ cm}}{(.0152)(.00174)} = \frac{1}{0} = \frac{1}{$$

Rt = 224.8 m2 = 7.02 m2

4) Ohmic bar (silver) = 3 (silver) dR = edl ~/em factor of 2 for both

(.00178)(2)(.0127+l Ton.640) sides of ohmic.

11.11 x10-3 I = (32.07 ma/cm²) (5.31 cm) l 1) 1' - (32.07)(5.31) (4.77×106) ddl (2)(.0017+)(.0127+lton 0.64) $\int_{\frac{b}{a}}^{c} \frac{x \, dx}{b^2} = \frac{x}{b} - \frac{a}{b^2} \ln \left(a + bx \right) / \frac{a}{b}$ 11 = 82.05 - 15,78 (ma.30 - In.049) 82.05 - 15.78 (-1.19 + 3.02) = 82.05 - 28.88 53.17 mu

g = 53.19 mil f = 64.84 m - 2 f = 54

SUMMARY OF RESISTANCE

 $R_{\rm B} = 3.4~{\rm m}\Omega$ - Base Material

 $R_{D} = 14.9 \text{ m}\Omega - \text{Diffused Layer}$

 $R_G = 7.0 \text{ m}\Omega - Grid Lines}$

 $R_{oh} = 64.8 \text{ m}\Omega - Ohmic Bar}$

 $\rm R_{T}$ = 3.4 + 14.9 + 2.0 + 64.8 = 90.1 $\rm m\Omega$ - Total Resistance

APPENDIX 2

SERIES RESISTANCE CALCULATIONS FOR INTERCONNECTS

Power loss due to resistance. Assume worst case 75°C, 0.8A

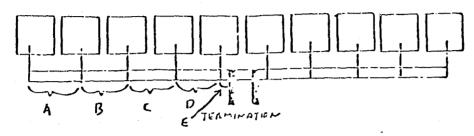
per cell.

.4" x 3 mil ribbon

8.25 Ω per 1000 ft.

.1" x 2 mil ribbon

49.5 Ω per 1000 ft.



Section	Length	Current	Power Loss
A	2.5"	0.8A	.00110W
В	2.5"	1.6A	.00440
С	2.5"	2.4A	.00990
D	2.5"	3.2A	.01761
E	1.3"	4.0A	.01431
			.04732

 \times 4 A-E segments per panel .18930W total power loss in bus bars.

200 1/4", 0.8A carrying interconnects .13200W power loss.

Total power loss .32130W or on 80W panel 0.40%

OF POOR QUALITY

sample calculation (Section A)

$$W_{L} = I^{2}R$$

$$W_{L} = (0.8)^{2} \times 8.25 \times \frac{1}{1000} \times \frac{1}{12} \times 2.5 A^{2} \cdot \Omega \cdot ft^{-1} \frac{ft}{in} \cdot in$$

$$W_{r.} = .00110W$$